Chemical Science

Accepted Manuscript

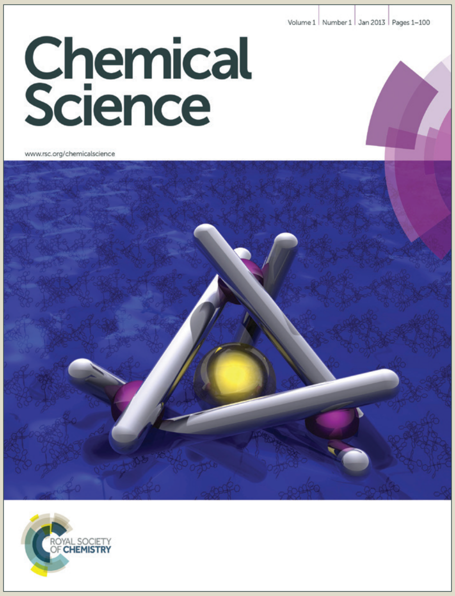

ROYAL SOCIETY OF CHEMISTRY

www.rsc.org/chemicalscience

Chemical Science

Dynamic Article Links ►

Cite this: DOI: 10.1039/c0xx00000x

www.rsc.org/xxxxxx

ARTICLE TYPE

Synthesis of various supramolecular hybrid nanostructures based on pillar[6]arene modified gold nanoparticles/nanorods and their application in pH- and NIR-triggered controlled release†

Yong Yao, Yang Wang and Feihe Huang*

Received (in XXX, XXX) Xth XXXXXXXXX 20XX, Accepted Xth XXXXXXXXX 20XX
DOI: 10.1039/b000000x

We have developed a new strategy to prepare various hybrid nanostructures based on host–guest interactions. Organic/inorganic supramolecular hybrid micelles, onion-like disks and vesicles were obtained by self-assembly of water-soluble pillar[6]arene **WP6** stabilized gold nanoparticles with different amounts of hydrophobic chain functionalized paraquat derivative **2** in water. Compared with the fabrication of hybrid nanostructures based on self-assembly of amphiphile stabilized metal nanoparticles, this supramolecular method can be used to prepare various hybrid nanostructures easily by only changing the amount of **2**, without the necessity to synthesize different amphiphilic stabilizers for different hybrid nanostructures. Furthermore, we prepared hybrid vesicles using **WP6** stabilized gold nanorods and **2**. These nanorod supramolecular hybrid vesicles were employed to encapsulate small molecules within their interiors under neutral conditions and release them in response to a pH decrease or NIR irradiation.

Introduction

In nature, organic and inorganic components intimately associate into well-organized hybrid structures to introduce various functions.[1] For example, nacre is composed of biological macromolecules and calcium carbonate nanocrystals which assemble structures with remarkable mechanical strength and toughness.[1b] Inspired by this, in the past decade, organic/inorganic hybrid nanostructures have aroused significant interest because of their collective properties and enhanced optical, electronic, and magnetic characteristics relative to those of individual nanoparticles (**NPs**), individual nanorods (**NRs**), and the corresponding organic stabilizers.[2] For instance, hybrid micelles can significantly enhance the stability of **NPs** in solution, which may facilitate their applications in catalysis, semiconductor manufacture, photonics, and biomimetic material fabrication.[2a] Hybrid vesicles can be disrupted by stimulus mechanisms inherent to either the stabilizers or the **NPs**.[2b] In regard to the fabrication of hybrid nanostructures, self-assembly of nanoparticles stabilized by amphiphiles represents a major strategy.[3] For examples, Liu and co-workers reported the synthesis of ultrasmall (< 4 nm) gold nanoparticles (**AuNPs**) stably anchored with a single amphiphilic triblock copolymer chain per nanoparticle and their controlled self-assembly into hybrid micelles, vesicles, rods, and large compound micelles.[3a] Duan and co-workers reported the manufacture of amphiphilic nanocrystals with mixed polymer brushes and their self-assembly into vesicular structures.[3b] The major disadvantage of this strategy is that one amphiphilic stabilizer can be used in the preparation of only one hybrid nanostructure. Consequently, it is challenging to develop a novel strategy to prepare various hybrid nanostructures using only one stabilizer. Herein, we demonstrated that host–guest interactions can be utilized to achieve this purpose.

As a new class of supramolecular hosts after crown ethers,[4] cyclodextrins,[5] calixarenes,[6] cucurbiturils,[7] and others,[8] pillar[*n*]arenes are useful and interesting macrocyclic compounds that present a hydrophobic core sandwiched between two functionalizable rims.[9,10] Their repeating units are connected by methylene bridges at the *para*-positions, forming a unique rigid pillar architecture. They can be easily chemically modified, making them promising candidates for applications in nanomaterials,[9l] molecular recognition,[9a,b,p] ion-transport,[9e] supramolecular polymers,[9c] *etc.* It was reported that the association constant between water-soluble pillar[6]arene **WP6** and paraquat is higher than 10^8 M^{-1} in water.[10e] In view of this, we proposed a new strategy for the easy fabrication of various hybrid nanostructures, such as micelles, onion-like disks, and vesicles, by self-assembly of **WP6** stabilized **AuNPs** with different amounts of hydrophobic chain functionalized paraquat

---

State Key Laboratory of Chemical Engineering,
Department of Chemistry, Zhejiang University, Hangzhou 310027,
P. R. China. E-mail: fhuang@zju.edu.cn; Fax: 86 571 8795 3189;
Tel: 86 571 8795 3189

† Electronic Supplementary Information (ESI) available: Synthetic procedures, characterizations. See DOI: 10.1039/b000000x/

derivative **2** (Scheme 1). More interestingly, supramolecular hybrid vesicles constructed from **WP6** stabilized gold nanorods (**AuNRs**) and **2** could be used to encapsulate small molecules within their interiors under neutral conditions and release them in response to a pH decrease or NIR irradiation.

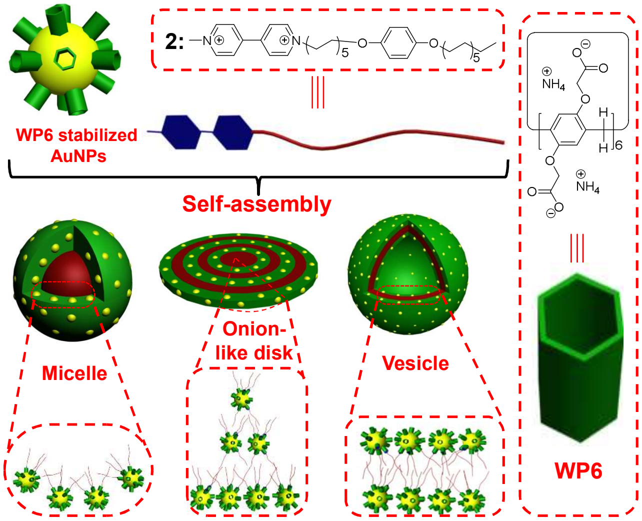

Scheme 1. Chemical structures of hydrophobic chain functionalized paraquat derivative **2** and water soluble pillar[6]arene **WP6** and schematic illustration of self-assembly of **WP6** stabilized gold nanoparticles and **2** into various hybrid nanostructures in water.

Results and discussion

Initially, **AuNPs** stabilized by **WP6** were synthesized by reducing $HAuCl_4$ (0.100 mL, 10.0 mM) with $NaBH_4$ (0.200 mL, 50.0 mM) in the presence of a series of selected concentrations of **WP6** (2.70 mL). The well-known surface plasmon resonance (SPR) of **AuNPs** was observed at ~520 nm (Fig. S7), suggesting the formation of **WP6** stabilized **AuNPs**.[11] Due to the increasing concentration of **WP6**, the SPR peak gradually underwent a blue shift from 560 to 520 nm, indicating smaller average gold nanoparticle diameters (Fig. S7).[6a,b] However, as shown in Fig. S7A (lines g, h and i), upon increasing the concentration of **WP6** from 0.400 mM to 0.800 mM, the SPR peak maximum remained the same in wavelength, indicating that the continuous addition of excess **WP6** had little influence on the average size of **AuNPs** after a certain amount was added. Therefore, when the concentration of **WP6** was 0.400 mM, the surfaces of **AuNPs** were almost completely covered with **WP6** and there was almost no excess **WP6** left. Here all the further studies on **AuNPs**, supramolecular amphiphilic gold nanoparticles (**SAuNPs**), and supramolecular hybrid nanostructures were based on **AuNPs** prepared with the concentration of **WP6** at 0.400 mM. As shown in Fig. S8, a transmission electron microscopy (TEM) image of **WP6** stabilized **AuNPs** and the histogram of size distribution of **AuNPs** were obtained. The average diameter and standard deviation determined from the histogram were 2.84 ± 0.32 nm. The TEM image revealed that **AuNPs** were spherical in shape with a relatively narrow particle size distribution and highly dispersed in water. What's more, the powder XRD pattern of **AuNPs** shows five diffraction peaks positioned at Bragg angles (2θ) between 30° and 90°, which can be attributed to the diffractions from five different gold lattice planes [(111), (200), (220), (311) and (222)] (Fig. S9).[6a]

For the fabrication of supramolecular hybrid nanostructures, **WP6** stabilized **AuNPs** were first prepared by dissolving $HAuCl_4$ (0.100 mL, 10.0 mM), **WP6** (2.70 mL, 0.400 mM) and $NaBH_4$ (0.200 mL, 50.0 mM) in water. Then an aqueous solution of **2** (2.70 mL, 0.0400 mM) was dropped into this solution. Because of the **WP6**/paraquat complexation, compound **2** encapsulated in **WP6** was deposited on the surfaces of the **AuNPs** to form **SAuNPs**, and these **SAuNPs** further self-assembled in water. To test the morphology of the assemblies (named No.1) made up of the combination of the **WP6** stabilized **AuNPs** and compound **2** in water, TEM and dynamic light scattering (DLS) studies were carried out. Fig. 1a showed that the assemblies were monodisperse. Furthermore, the DLS results revealed that the average size of the assemblies was about 3.2 nm (Fig. S10b), close to that of original **WP6** stabilized **AuNPs** (2.7 nm) (Fig. S10a). The reason might be that the hydrophilic parts of the **SAuNPs** are much bigger than their hydrophobic parts, so these **SAuNPs** were almost hydrophilic and monodisperse in water.

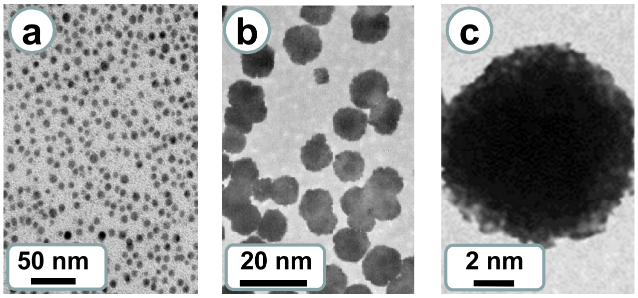

Fig. 1 TEM images of supramolecular amphiphilic gold nanoparticles self-assembled in water: (a) No.1, [**WP6**]/**2** = 10:1; (b) No.2, [**WP6**]/**2** = 4:1. (c) Enlarged image of b.

We then increased the concentration of compound **2** to 0.100 mM while other conditions remained unchanged. At this concentration, the ratio between **WP6** and **2** was about 4:1, so the hydrophobic parts of **SAuNPs** became bigger than those in the assemblies No.1. Consequently, the **SAuNPs** tended to self-assemble to form micelles with the **WP6** stabilized **AuNPs** as the coronas and the hydrophobic groups as the cores (Scheme 1, named No.2). The average extended length of **WP6** stabilized **AuNPs** complexed with one molecule of compound **2** was about 6.0 nm, so the average diameter of the assembled aggregates was around 12 nm theoretically. As shown in Fig. 1b, TEM images showed spherical micelles and their average size was about 10 nm in diameter, in accord with the DLS result (Fig. S11). It should be pointed out that the average diameter of the micelles measured by DLS was a little larger than that obtained from the TEM images, attributable to swelling of the spherical structures in water.[9k] Owing to the hydrophobicity of the cores of the nanoparticle hybrid micelles, hydrophobic molecules could be encapsulated in the micelles. Moreover, as demonstrated previously,[10e] the COO^- groups of the **WP6** host can be converted into the neutral carboxylic acid groups by adding acid, destroying the complexation between **WP6** and the viologen dication of **2**. As a result, the micellar structure was destroyed (Fig. S15). At the same time, the encapsulated hydrophobic molecules Nile Red were released (Fig. S16).

In the next stage, the concentration of **2** was increased to 0.150 mM. On this occasion, the ratio between **WP6** and **2** is about 2.7:1 and the hydrophobic parts of the **SAuNPs** were further increased. DLS studies showed that the average diameter of the assemblies (named No. 3) was ~250 nm, which was much bigger than the above mentioned assemblies (No. 2). As shown by the SEM image in Fig. 2a, the morphology of the **SAuNPs** (No. 3) self-assembled in water changed from spherical micelles to uniformly dispersed disk-like structures, and the average diameter was ~250 nm, in accord with the DLS result (Fig. S12). Furthermore, the TEM image (Fig. 2b) of one disk indicated that it was actually a multi-layer onion-like micelle. The structural transition from spherical micelles to onion-like disks might be driven by increased interfacial tension. In this regime the interfacial tension became so large as to overwhelm the other free energy terms, giving rise to complete stretching of the core and a flat interface.[12]

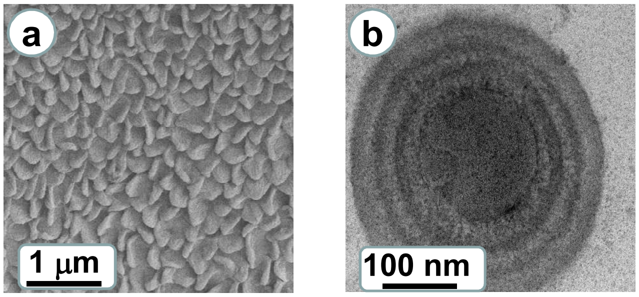

Fig. 2 (a) SEM image and (b) TEM image of supramolecular amphiphilic gold nanoparticles (No.3, [**WP6**]/**2** = 2.7:1) self-assembled in water.

After that, the concentration of **2** was further raised to 0.250 mM in order to further increase the hydrophobic parts of the **SAuNPs**. Subsequently, another interesting morphology (named No. 4) was generated by self-assembly of the **SAuNPs** ([**WP6**]/**2** = 1.6:1) in water. SEM images (Fig. 3a and b) showed the typical vesicle morphology of hollow spheres composed of an inside cavity and an outer thick wall, and the vesicles were around 400 nm in diameter and thus in agreement with the DLS result (Fig. S13). A typical collapsed aggregate (Fig. 3b) clearly showed that the assemblies were hollow. TEM images also showed the formation of the vesicles whose average size was consistent with the SEM results. From an enlarged TEM image we can clearly see **AuNPs** on the surface of the vesicle (Fig. 3d). Moreover, the average thickness of the vesicle wall was roughly 10 nm (Fig. S14), which was just about the diameter of the previous micelles, indicating the bilayer wall structure of the vesicle (Scheme 1). A mechanism was proposed to explain why the morphological transition from micelles to vesicles. The micro-assembled structure of the aggregates formed by amphiphiles is determined by the curvature of the membrane.[10e] Due to the more extensive hydrophobic parts of the **SAuNPs** relative to the hydrophilic parts under this condition, the steric hindrance became greater, so a vesicular structure with low curvature formed.[10e]

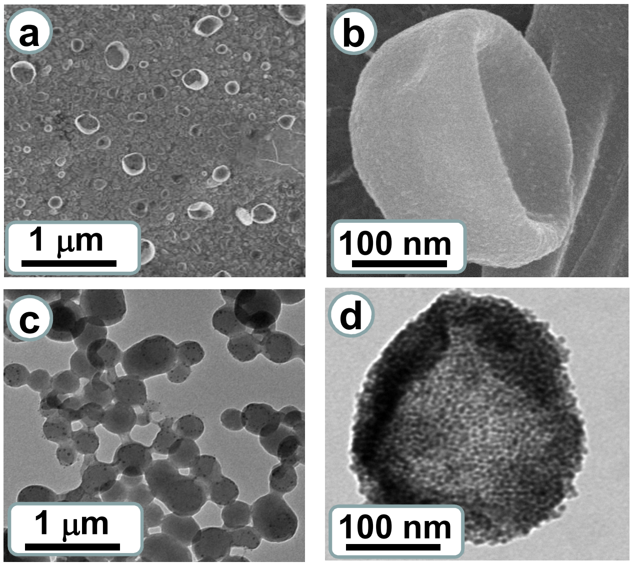

Fig. 3 (a) SEM image and (c) TEM image of supramolecular amphiphilic gold nanoparticles (No.4, [**WP6**]/**2** = 1.6:1) self-assembled in water. (b) Enlarged SEM image and (d) enlarged TEM image of a typical nanoparticle supramolecular hybrid vesicle.

In contrast to the hybrid micellar aggregates, vesicles can encapsulate hydrophilic molecules within their interiors under neutral conditions and release these molecules in response to a pH decrease. On the basis of this, calcein as a hydrophilic fluorescent molecule was put into the vesicle solution. As shown in Fig. S17, release of calcein from the interiors of the vesicles was accompanied by an increase in fluorescence emission upon adding acid (aqueous HCl). These pH-responsive nanocapsules might have potential applications in selective drug delivery in tissues with a lower pH, such as infected tissues and tumor tissues.[13]

It is well known that **AuNPs**/**AuNRs** can rapidly convert the light absorbed at their SPR wavelengths into thermal energy to heat up the surrounding medium.[14] This photothermal conversion property has attracted tremendous attention in the development of hybrid nanomaterials for photothermal therapy[15] and remotely controlled drug delivery.[16] Particularly for *in vivo* applications, nanostructures with SPR bands in the NIR spectral window are highly desirable because of the smaller extent of attenuation of light by blood and soft tissues in this spectral range.[17] However, for this purpose, **AuNPs** with SPR at ~540 nm (Figs. S7, and 4b, line I) could not convert near-infrared light into thermal energy. Therefore, here we utilized **WP6** stabilized **AuNRs** (~6 nm × 20 nm, Figs. 4a, S18, and S19), whose longitudinal plasmon resonance can be easily tuned into the NIR region by variation of their aspect ratio, and **2** to prepare supramolecular hybrid vesicles.[15a,d] Fig. 4c shows that nanorod supramolecular hybrid vesicles with diameters of ~500 nm were successfully obtained when [**WP6**]/**2** = 1.6:1. UV−Vis spectrometry (Fig. 4b, lines II and III) showed that in the nanorod hybrid vesicles, both the transverse and longitudinal plasmon resonances of the **AuNRs** were red-shifted and became broader because of the strong plasmonic coupling of nanorods in close proximity. Next, we tested the NIR-induced deconstruction of the nanorod hybrid vesicles by irradiating a drop of vesicle dispersion on a substrate with a 785 nm diode laser at 2 W/cm^2. TEM observation (Fig. 4d) revealed that the nanorod hybrid vesicles lost their spherical morphology after 2 min of irradiation and were disrupted into irregular aggregates, confirming that the localized heating generated by the assembled **AuNRs** was sufficient to induce the supramolecular hybrid vesicles to collapse. Furthermore, calcein was encapsulated into the supramolecular hybrid vesicles under neutral conditions. The release of calcein molecules after 2 min of NIR irradiation also confirmed the NIR-trigged collapse of these hybrid vesicles (Figs. 4e and S20). What is more, these nanorod hybrid vesicles could also encapsulate hydrophilic molecules within their interiors under neutral conditions and released them in response to a pH decrease (Fig. S21).

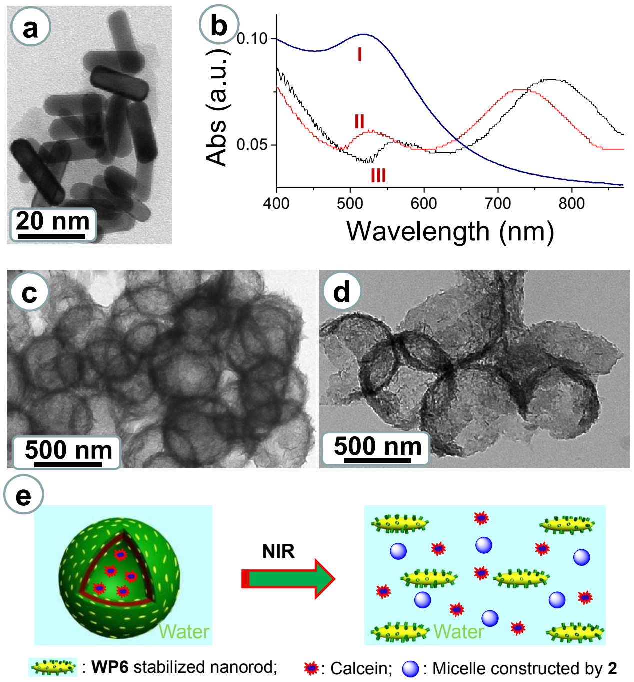

Fig. 4 (a) TEM image of **WP6** stabilized gold nanorods. (b) UV–Vis spectra of **WP6** stabilized gold nanoparticles prepared when [**WP6**] = 0.400 mM (line I), **WP6** stabilized gold nanorods (line II), and nanorod supramolecular hybrid vesicles (line III). (c) TEM image of the nanorod supramolecular hybrid vesicles. (d) TEM image of the vesicles after 2 minutes of irradiation with a 785 nm laser. (e) Schematic representation of a NIR-triggered vesicle-to-micelle transition and the subsequent release of encapsulated calcein.

Conclusions

In summary, we have developed a novel and efficient method for the fabrication of various hybrid nanostructures through host–guest interactions. Organic/inorganic supramolecular hybrid micelles, onion-like disks and vesicles were obtained by self-assembly of **WP6** stabilized **AuNPs** with different amounts of **2** in water. The nanoparticle hybrid micelles were used to encapsulate and release hydrophobic molecules, while the nanoparticle hybrid vesicles were used to encapsulate and release hydrophilic molecules. In contrast to other hybrid structures, the disruption of the supramolecular hybrid structures can be triggered by stimulus mechanisms inherent to either the host–guest interactions or the nanocrystals. Therefore, the hybrid vesicles constructed from **WP6** stabilized **AuNRs** and **2** encapsulated small molecules within their interiors under neutral conditions and released them in response to a pH decrease or NIR irradiation. This new method can be used in the preparation of various hybrid nanostructures with various functions and easily expanded to other metal nanocrystals and other noncovalent interactions. The development of supramolecular hybrid nanostructures based on stimuli-responsive host–guest interactions can enable their broad applications in biosensing, multimodality imaging, and theranostic nanomedicine.

Acknowledgements

This work was supported by National Basic Research Program (2013CB834502), the National Natural Science Foundation of China (21125417), and the Fundamental Research Funds for the Central Universities.

Notes and references

1 (*a*) H. Zhai, W. Jiang, J. Tao, S. Lin, X. Chu, X. Xu and R. Tang, *Adv. Mater.*, 2010, **22**, 3729; (*b*) Y. Quan, H. Zhai, Z. Zhang, X. Xu and R. Tang, *CrystEngComm*., 2012, **14**, 7184.

2 (*a*) L. B. Wang, L. G. Xu, H. Kuang, C. L. Xu and N. A. Kotov, *Acc. Chem. Res.*, 2012, **45**, 1916; (*b*) J. He, Z. Wei, L. Wang, Z. Tomova, T. Babu, C. Wang, X. Han J. T. Fourkas and Z. Nie, *Angew. Chem., Int. Ed.*, 2013, **52**, 2463.

3 (*a*) J. Hu, T. Wu, G. Zhang and S. Liu, *J. Am. Chem. Soc.*, 2012, **134**, 7624; (*b*) J. Song, L. Cheng, A. Liu, J. Yin, M. Kuang and H. Duan, *J. Am. Chem. Soc.*, 2011, **133**, 10760; (*c*) J. He, X. Huang, Y.-C. Li, Y. Liu, T. Babu, M. A. Aronova, S. Wang, Z. Lu, X. Chen and Z. Nie, *J. Am. Chem. Soc*., 2013, **135**, 7974.

4 (*a*) F. Huang, F. R. Fronczek and H. W. Gibson, *J. Am. Chem. Soc.*, 2003, **125**, 9272; (*b*) F. Huang, D. S. Nagvekar,C. Slebodnick and H. W. Gibson, *J. Am. Chem. Soc.*, 2005, **127**, 484; (*c*) Y. Liu, A. Bruneau, J. He and Z. Abliz, *Org. Lett.*, 2008, **10**, 765; (*d*) Z. Niu and H. W. Gibson, *Chem. Rev.*, 2009, **109**, 6024; (*e*) W. Jiang, A. Schäfer, P. C. Mohr and C. A. Schalley, *J. Am. Chem. Soc.*, 2010, **132**, 2309; (*f*) Z. Niu, F. Huang and H. W. Gibson, *J. Am. Chem. Soc.*, 2011, **133**, 2836; (*g*) K. Zhu, V. N. Vukotic and S. J. Loeb, *Angew. Chem., Int. Ed.*, 2012, **51**, 2168; (*h*) Z. Qi, P. M. Molina, W. Jiang, Q. Wang, K. Nowosinski, A. Schulz, M. Gradzielski and C. A. Schalley, *Chem. Sci.*, 2012, **3**, 2073; (*i*) K. Zhu, V. N. Vukotic, N. Noujeim and S. J. Loeb, *Chem. Sci.*, 2012, **3**, 3265; (*j*) R. Sun, C. Xue, X. Ma, M. Gao, H. Tian and Q. Li, *J. Am. Chem. Soc.*, 2013, **135**, 5990; (*k*) Y. Ding, P. Wang, Y.-K. Tian, Y.-J. Tian and F. Wang, *Chem. Commun.*, 2013, **49**, 5951; (*l*) Y.-K. Tian, Z.-S. Yang, X.-Q. Lv, R.-S. Yao and F. Wang, *Chem. Commun.*, 2014, DOI: 10.1039/C4CC03158J.

5 (*a*) A. Mirzoian and A. E. Kaifer, *Chem. Commun.*, 1999, 1603; (*b*) A. Harada, *Acc. Chem. Res.* 2001, **34**, 456; (*c*) J. Terao, A. Tang, J. J. Michels, A. Krivokapic and H. L. Anderson, *Chem. Commun.*, 2004, 56.

6 (*a*) Y. Sun, C-G. Yan, Y. Yao, Y. Han and M. Shen, *Adv. Funct. Mater.*, 2008, **18**, 3981; (*b*) Y. Sun, Y. Yao, C.-G. Yan, Y. Han and M. Shen, *ACS Nano*, 2010, **4**, 2129; (*c*) D.-S. Guo and Y. Liu, *Chem. Soc. Rev.*, 2012, **41**, 5907.

7 (*a*) Y. J. Jeon, H. Kim, S. Jon, N. Selvapalam, D. H. Seo, I. Oh, C.-S. Park, S. R. Jung, D.-S. Koh and K. Kim, *J. Am. Chem. Soc.*, 2004, **126**, 15944; (*b*) N.-F. She, M. Gao, X.-G. Meng, G.-F. Yang, J. A. A. W. Elemans, A.-X. Wu and L. Isaacs, *J. Am. Chem. Soc.*, 2009, **131**, 11695; (*c*) Y. Lan, X. J. Loh, J. Geng, Z. Walsh and O. A. Scherman, *Chem.*

Commun., 2012, **48**, 8757; (*d*) J. B. Wittenberg, P. Y. Zavalij and L. Isaacs, *Angew. Chem. Int. Ed.,* 2013, **52**, 3690.

8 (*a*) A. Altieri, V. Aucagne, R. Carrillo, G. J. Clarkson, D. M. D'Souza, J. A. Dunnett, D. A. Leigh and K. M. Mullen, *Chem. Sci.*, 2011, **2**, 1922; (*b*) D. A. Leigh, P. J. Lusby, A. M. Z. Slawin and D. B. Walker, *Chem. Commun.*, 2012, **48**, 5826; (*c*) G. Wu, P. Verwilst, K. Liu, M. Smet, C. F. J. Faulc and X. Zhang, *Chem. Sci.,* 2013, **4**, 4486; (*d*) A. V. Quaethem, P. Lussis, D. A. Leigh, A.-S. Duwez and C.-A. Fustin, *Chem. Sci.,* 2014, **5**, 1449.

9 Selected publications about pillar[5]arenes: (*a*) T. Ogoshi, S. Kanai, S. Fujinami, T. A. Yamagishi, Y. Nakamoto, *J. Am. Chem. Soc.,* 2008, **130**, 5022; (*b*) C. Li, L. Zhao, J. Li, X. Ding, S. Chen, Q. Zhang, Y. Yu and X. Jia, *Chem. Commun.,* 2010, **46**, 9016; (*c*) Z. Zhang, Y. Luo, J. Chen, S. Dong, Y. Yu, Z. Ma and F. Huang, *Angew. Chem., Int. Ed.,* 2011, **50**, 1397; (*d*) N. L. Strutt, R. S. Forgan, J. M. Spruell, Y. Y. Botros and J. F. Stoddart, *J. Am. Chem. Soc.,* 2011, **133**, 5668; (*e*) W. Si, L. Chen, X.-B. Hu, G. Tang, Z. Chen, J.-L. Hou and Z.-T. Li, *Angew. Chem., Int. Ed.,* 2011, **50**, 12564; (*f*) I. Nierengarten, S. Guerra, M. Holler, J.-F. Nierengarten and R. Deschenaux, *Chem. Commun.,* 2012, **48**, 8072; (*g*) Y. Yao, M. Xue, J. Chen, M. Zhang and F. Huang, *J. Am. Chem. Soc.,* 2012, **134**, 15712; (*h*) T. Nishimura, Y. Sanada, T. Matsuo, T. Okobira, E. Mylonas, N. Yagi and K. Sakurai, *Chem. Commun.*, 2013, **49**, 3052; (*i*) Y. Fang, L. Wu, J. Liao, L. Chen, Y. Yang, N. Liu, L. He, S. Zou, W. Feng and L. Yuan, *RSC Adv.*, 2013, **3**, 12376; (*j*) H. Zhang, K. T. Nguyen, X. Ma, H. Yan, J. Guo, L. Zhu and Y. Zhao, *Org. Biomol. Chem.*, 2013, **11**, 2070; (*k*) G. Yu, Y. Ma, C. Han, Y. Yao, G. Tang, Z. Mao, C. Gao and F. Huang, *J. Am. Chem. Soc.,* 2013, **135**, 10310; (*l*) Y. Yao, M. Xue, Z. Zhang, M. Zhang, Y. Wang and F. Huang, *Chem. Sci*., 2013, **4**, 3667; (*m*) S. Dong, B. Zheng, Y. Yao, C. Han, J. Yuan, M. Antonietti and F. Huang, *Adv. Mater.,* 2013, **25**, 6864; (*n*) X. Wang, K. Han, J. Li, X. Jia and C. Li, *Polym. Chem*., 2013, **4**, 3998; (*o*) J.-F. Xu, Y.-Z. Chen, L.-Z. Wu, C.-H. Tung and Q.-Z. Yang, *Org. Lett.,* 2013, **15**, 6148; (*p*) C. Li, J. Ma, L. Zhao; Y. Zhang, Y. Yu, X. Shu, J. Li and X. Jia, *Chem. Commun.*, 2013, **49**, 1924; (*q*) X. Shu, W. Chen, D. Hou, Q. Meng, R. Zheng and C. Li, *Chem. Commun.*, 2014, **50**, 4820; (*r*) Y. Yao, X. Chi, Y. Zhou and F. Huang, *Chem. Sci.,* 2014, **5**, 2778; (*s*) W. Si, Z.-T. Li and J.-L. Hou, *Angew. Chem. Int. Ed.*, 2014, **53**, 4578.

10 Selected publications about pillar[*n*]arenes ($n > 5$): (*a*) D. Cao, Y. Kou, J. Liang, Z. Chen, L. Wang and H. Meier, *Angew. Chem., Int. Ed.,* 2009, **48**, 9721; (*b*) C. Han, F. Ma, Z. Zhang, B. Xia, Y. Yu and F. Huang, *Org. Lett.,* 2010, **12**, 4360; (*c*) G. Yu, C. Han, Z. Zhang, J. Chen, X. Yan, B. Zheng, S. Liu and F. Huang, *J. Am. Chem. Soc.,* 2012, **134**, 8711; (*d*) G. Yu, M. Xue, Z. Zhang, J. Li, C. Han and F. Huang, *J. Am. Chem. Soc.,* 2012, **134**, 13248; (*e*) G. Yu, X. Zhou, Z. Zhang, C. Han, Z. Mao, C. Gao and F. Huang, *J. Am. Chem. Soc.,* 2012, **134**, 19489; (*f*) T. Ogoshi, K. Kida and T. A. Yamagishi, *J. Am. Chem. Soc.,* 2012, **134**, 20146; (*g*) Q. Duan, Y. Cao, Y. Li, X. Hu, T. Xiao, C. Lin, Y. Pan, and L. Wang, *J. Am. Chem. Soc.*, 2013, **135**, 10542; (*h*) W. Xia, X.-Y. Hu, Y. Chen, C. Lin and L. Wang, *Chem. Commun.*, 2013, **49**, 5085; (*i*) Y. Yao, K. Jie, Y. Zhou and M. Xue, *Chem. Commun.*, 2014, **50**, 5072

11 H. Li, D.-X. Chen, Y.-L. Sun, Y. B. Zheng, L.-L. Tan, P. S. Weiss,and Y.-W. Yang, *J. Am. Chem. Soc.*, 2013, **135**, 1570.

12 X. Ji, S. Dong, P. Wei, D. Xia and F. Huang, *Adv. Mater.*, 2013, **25**, 5725.

13 M. Lee, S-J. Lee and L-H. Jiang, *J. Am. Chem. Soc.,* 2004, **126**, 12724.

14 P. K. Jain, X. H. Huang, I. H. El-Sayed and M. A. El-Sayed, *Acc. Chem. Res.*, 2008, **41**, 1578.

15 (*a*) X. H. Huang, I. H. El-Sayed, W. Qian and M. A. El-Sayed, *J. Am. Chem. Soc.,* 2006, **128**, 2115; (*b*) J. Y. Chen, D. L. Wang, J. F. Xi, L. Au, A. Siekkinen, A. Warsen, Z. Y. Li, H. Zhang, Y. N. Xia and X. D. Li, *Nano Lett.,* 2007, **7**, 1318; (*c*) J. You, G. D. Zhang and C. Li, *ACS Nano,* 2010, **4**, 1033; (*d*) G. von Maltzahn, J. H. Park, A. Agrawal, N. K. Bandaru, S. K. Das, M. J. Sailor and S. N. Bhatia, *Cancer Res.,* 2009, **69**, 3892.

16 (*a*) K. W. Hu, T. M. Liu, K. Y. Chung, K. S. Huang, C. T. Hsieh, C. K. Sun and C. S. Yeh, *J. Am. Chem. Soc.,* 2009, **131**, 14186; (*b*) Y. D. Jin and X. H. Gao, *J. Am. Chem. Soc.,* 2009, **131**, 17774; (*c*) T. R. Kuo, V. A. Hovhannisyan, Y. C. Chao, S. L. Chao, S. J. Chiang, S. J. Lin, C. Y. Dong and C. C. Chen, *J. Am. Chem. Soc.,* 2010, **132**, 14163; (*d*) R. Huschka, O. Neumann, A. Barhoumi and N. J. Halas, *Nano Lett.,* 2010, **10**, 4117.

17 J. V. Frangioni, *Curr. Opin. Chem. Biol.,* 2003, **7**, 626.

TOC

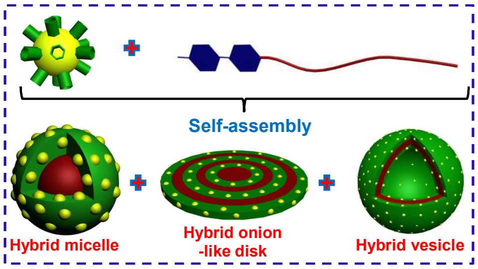

Organic/inorganic supramolecular hybrid micelles, onion-like disks and vesicles were obtained by self-assembly of water-soluble pillar[6]arene stabilized gold nanoparticles/nanorods with different amounts of a hydrophobic chain functionalized paraquat derivative in water. These hybrid nanostructures can be used in pH- and NIR-triggered controlled release.